European Polymer Journal 44 (2008) 3941–3945

Contents lists available at ScienceDirect

European Polymer Journal

journal homepage: www.elsevier.com/locate/europolj

Macromolecular Nanotechnology

Optical transparency in a polymer blend induced by clay nanofillers

Antonios Kelarakis [a,*], Kyunghwan Yoon [b]

[a] National and Kapodistrian University of Athens, Department of Chemistry, Physical Chemistry Laboratory, 157 71 Panepistimiopolis, Athens, Greece
[b] Department of Chemistry, Stony Brook University, Stony Brook, NY 11794-3400, USA

ARTICLE INFO

Article history:
Received 22 May 2008
Received in revised form 8 August 2008
Accepted 17 August 2008
Available online 2 September 2008

Keywords:
Nanocomposites
Nanoclays
Polymer blend
Optical transparency

ABSTRACT

The effect of added nanoclays to the morphological characteristics and the macroscopic properties in a blend of isotactic polypropylene (iPP) and poly(ethylene oxide) (PEO) is examined in this study. It is shown that strong interactions between the surfactant used for clay modification and the binary matrix can effectively control the spatial organization of the suspended polymer droplets. It is also shown that the emulsifying efficiency of nanoclays to the polymer blend has a critical effect on the macroscopic properties of the nanocomposites. In this study, we present a unique case in which the incorporation of a small amount of organically modified nanoclay induces a dramatic transformation from an opaque to a transparent system.

1. Introduction

The emulsifying efficiency and the compatibilization action of the organically modified silicate platelets to miscible [1] and immiscible [2–13] blends have been well established. The shrinkage of the suspended droplets within the continuum of the major component of the polymer blend as a consequence of nanoclay dispersion has been probed by microscopy imaging (SEM, TEM, and AFM) in several reports [2–13]. It has been recently demonstrated [12] that the degree of chemical affinity in the organic/inorganic interface is a critical factor determining the size of the phase-separated domains (in a typical pair of incompatible polymers), which in turn has a profound impact on the macroscopic properties (rheological response, mechanical performance) of the nanocomposites. In a recent study, the remarkable mechanical properties of a clay reinforced poly(vinylidene fluoride/nylon-6 (PVDF/N6) have been related to the degree of clay dispersion and the location of nanoadditives [13].

Here, we focus on a specific application of the nanoadditive controlled spatial organization, in which the incorporation of a small amount of silicate platelets to a polymer blend results in a transition from an opaque to a transparent system. In other words, the emulsifying effects of organoclays can be manifested directly not only microscopically, but also macroscopically, given that the induced transparency can be observed by bare eye.

In this study, we selected isotactic polypropylene (iPP)/poly(ethylene oxide) (PEO) blends, a pair of typically immiscible polymers. Quaternary ammonium compounds of Montmorillonite (MNT) clays modified with two different surfactants (one with hydrocarbon chains and one with –OH groups attached to the aliphatic backbone) were used as nanofillers. The resulting ternary systems were then characterized by X-ray diffraction (XRD), Differential Scanning Calorimetry (DSC), rheology, Optical Microscopy, Scanning Electron Microscopy (SEM) and UV–Visible spectrometry and compared with the corresponding unfilled blend.

2. Experimental section

2.1. Preparation of the nanocomposites

Poly(ethylene oxide) (PEO), $M_n = 10^5$ g/mol and isotactic polypropylene (iPP), $M_w = 1.9 \times 10^5$ g/mol, $M_n = 5 \times 10^4$

* Corresponding author. Tel.: +30 2107274562.
E-mail address: akelar@cc.uoa.gr (A. Kelarakis).

0014-3057/$ - see front matter © 2008 Elsevier Ltd. All rights reserved.
doi:10.1016/j.eurpolymj.2008.08.030

g/mol, melt index = 35 were purchased by Sigma–Aldrich Co. Two organically modified montmorillonites (MMT) clays were used in this study; I.30T from Nanocor Inc. is a octadecyltrimethyl ammonium exchanged MMT (apolar character) and Cloisite 30B from Southern Clay Products, a bis(hydroxyethyl)methyl tallow ammoniun exchanged MMT (polar character).

Prior to nanocomposites preparation, all materials were dried in a vacuum oven overnight. 70:30 iPP/PEO blends were prepared, while filled samples contained 5 wt% clay. The components were first thoroughly mixed in a Flack-Tek DAC-150 FV speed mixer, before being melt coextruded with a twin screw at 200 °C under nitrogen flow (for 5 min). Specimens with ring shape were prepared by a Daca Instruments microinjector with the barrel at 220 °C, the mold at room temperature and the injection pressure at 690 kPa.

3. Methods

Wide-angle, X-ray diffraction (WAXS) spectra of the materials studied were recorded at room temperature using a Scintag Inc. θ–θ goniometer (Cu Kα radiation, λ = 1.54 Å). The thermographs of the samples were obtained by a TA Instrument Q1000 series calorimeter over the temperature range −50 to 200 °C at a scan rate of 10 °C/min. Rheological properties of the nanocomposites were determined using a Paar Physica Modular Compact Rheometer 300 (MCR 300) equipped with parallel plate geometry (diameter 25 mm). Measurements were performed in small amplitude oscillatory shear, at a fixed temperature of 200 °C, in a dry nitrogen atmosphere to suppress oxidative degradation. The samples were kept for 30 min in the rheometer for thermal equilibrium and structural relaxation, before any measurements were performed. The visible spectra of the samples were acquired by a Perkin Elmer UV/visible spectrometer (λ = 10).

For optical microscopy, the molten samples were squeezed between two cover glasses in a Metler FP82 HT hot-stage. The samples were heated up to 200 °C for 10 min and then quenched to room temperature. The images were obtained using a Nikon Eclipse E600 POL optical microscope. Morphologies of cryogenically fractured samples were studied using a Leica stereoscan model 440 SEM. All samples were gold coated in order to reduce charge effects.

4. Results and discussion

XRD patterns of the two nanocomposites are shown in Fig. 1 together with the corresponding patterns of the dry clays. The expansion of the interlayer galleries of the silicate particles in the composites compared to the basal spacing of the neat clays is indicative of intercalated structures. The broad peak at around 2.2° that appears more pronounced for 30B filled sample indicates a higher degree of order for that nanocomposite, an effect that can be assigned to the higher affinity of the more polar 30B clay to PEO. It should be noted, however, that none hybrid shows a well-ordered intercalated structure, an effect that points

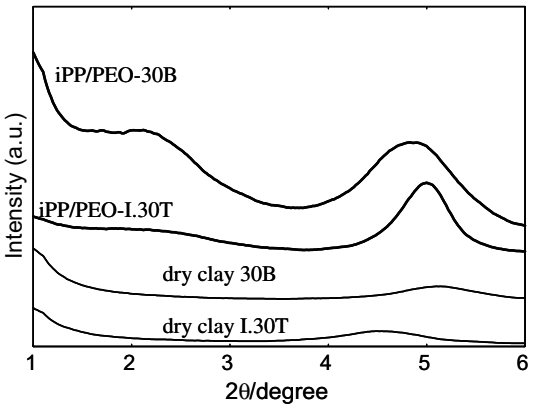

Fig. 1. XRD patterns of the iPP/PEO blend based nanocomposites filled with; (a) clay I.30T and (b) clay 30B.

out to the inherent incompatibility of the two polymer components. The XRD spectra at higher angles (data not shown here) revealed that the incorporation of clay nanoparticles does not cause any changes to the crystalline structure of the components. In particular, the crystal reflections identified for polypropylene can be indexed in all samples considered as the crystalline structure of the α-monoclinic form of iPP [14].

DSC thermographs of the nanocomposites are compared with the corresponding plot of the neat blend in Fig. 2a. All the samples showed two distinct crystallization regions, as a result of the immiscibility of the two polymer components at the molecular level. In particular, the crystallization temperature (T_{cr}) of iPP was found to be 114.4, 113.3, and 111.3 °C for the unfilled, the I.30T and the 30B filled blend, respectively. At the same time, the multiple peak of the PEO crystallization observed for the unfilled blend points out to the phenomenon of fractioned crystallization in polymer blends [15]. The addition of clay nanoparticles drastically suppresses this effect. It is our opinion that the non-fractionated crystallization of PEO observed for nanocomposites, as opposed to the unfilled blend, indicates that polymer–polymer interface has been reduced upon addition of clay nanoparticles (despite the improved dispersion), implying that a certain amount of nanoparticles is located to the polymer–polymer interface, thus minimizing iPP–PEO interactions. It should be noted, however, that the incorporation of nanoclays does not change the crystallinity index of either iPP or PEO, when examined in their neat state (not blended).

In some cases, it has been supported [16–18] that the clay layers dispersed in a PEO matrix can delay the spherulite growth by promoting the amorphous phase in the vicinity of the silicate surface, an effect that has been assigned to a cation-ethylene oxide coordination that defects the helical PEO arrangement [19]. Nevertheless, in the present study it was found that the incorporation of silicate layers in PEO matrix does not influence the crystallization parameters of this homopolymer. This can be clearly seen in Fig. 2b that shows DSC exothermic graphs for the pure PEO together with PEO-I.30T and PEO-30B clay nanocomposites. It can be seen that T_{cr} = 48.1 °C for all three

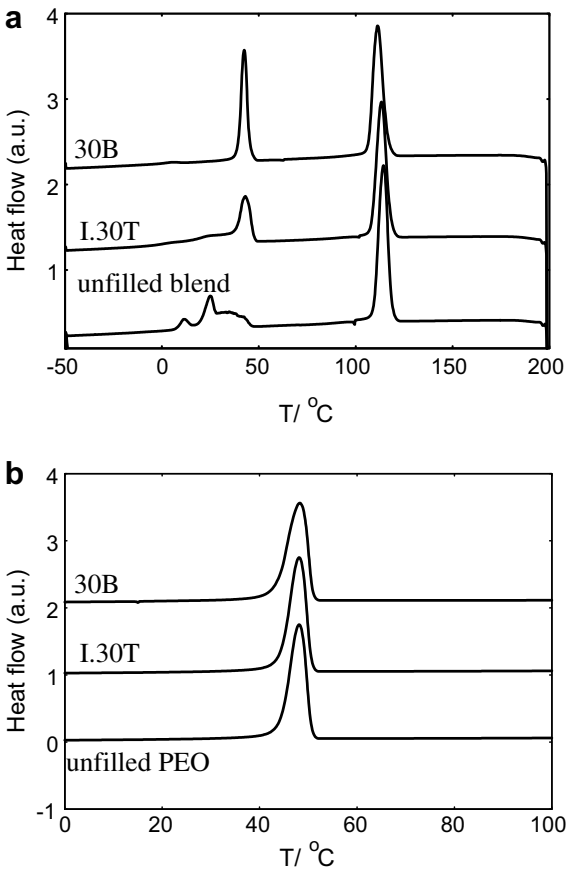

Fig. 2. DSC thermographs; (a) the unfilled blend and the corresponding clay filled samples (b) the unfilled PEO and the corresponding nanocomposites.

samples and that the crystallinity index of PEO is not affected by the presence of clay.

The viscoelastic response of the nanocomposite melts and the unfilled blend at $T = 200\ ^{\circ}C$ is demonstrated in Fig. 3. Compared to the unfilled blend, 30B nanocomposite showed increased values of both storage G' and loss G'' moduli within the entire frequency window, while the addition of I.30T leaves the rheological characteristics of the neat blend essentially unchanged. Pronounced deviations from the ideal melt behavior, particular in the low frequency region, are typical for several classes of nanocomposites [12,20–22] that exhibit pseudo-solid like behavior. In these physical gels, the long-range connectivity arises from the cross-linking formation (physical in nature) induced by nanofillers. As a result of this physical cross-linking, 30B filled sample shows $G' > G''$ at all frequencies, while the unfilled sample and the I.30T nanocomposite exhibit rheological behavior similar to an entangled polymer melt, having short relaxation time.

Additional rheological tests demonstrated that the viscosity of PEO melt was considerably increased by addition of 30B, but remained essentially the same upon addition of I.30T. This observation indicates that PEO interacts more favorably with 30B compared to I.30T. It also implies that

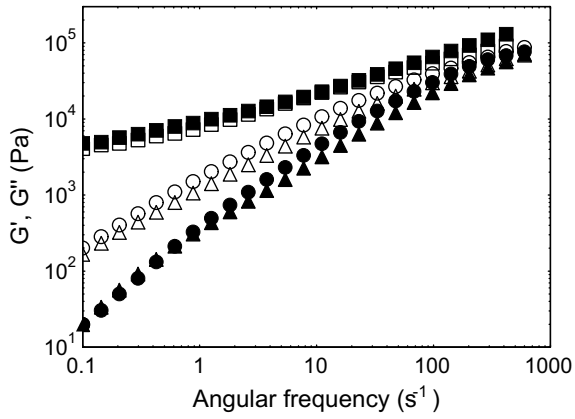

Fig. 3. Frequency dependence of storage (G') and loss (G'') modulus for the unfilled blend (△), the 5 wt% I.30T (□) and the 5 wt% 30B nanocomposites (○) at $T = 200\ ^{\circ}C$. Filled symbols denote G' and unfilled symbols denote G''.

addition of 30B can effectively increase the viscosity ratio of dispersed over matrix phase (η_d/η_m), in which case reduced domain sizes are expected [13,23].

Incorporation of 5 wt% 30B clay to the polymer blend causes a dramatic transformation from an opaque to an optical transparent system, as is evident in Fig. 4, in which both samples have the same thickness (0.15 cm). At the same time, introduction of 5 wt% of clay I.30T only improves slightly the transparency of the blend, thus this sample was not included in Fig. 4. In order to set a quantified level of transparency for the unfilled blend and the two nanocomposites, the visible spectra of these samples were recorded. As presented in Fig. 5, the absorbance of the system is reduced by a factor of 3 in the case of 30B filled nanocomposite, but is little affected by the introduction of I.30T clay.

Optical microscopy (Fig. 6) and SEM images (Fig. 7) provide an estimation of the domain size of the minor phase in these three systems. Micrographs 6a and 7a were derived

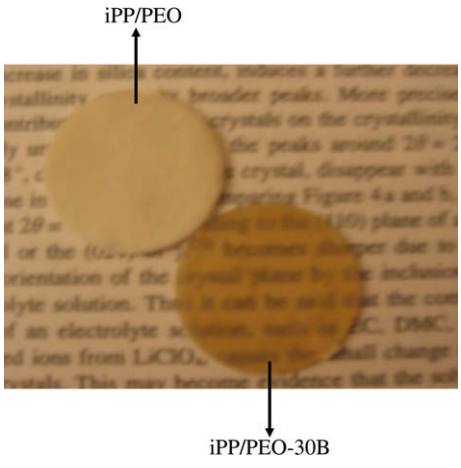

Fig. 4. Photographs of the unfilled blend and the 30B nanocomposite, demonstrating a dramatic difference of the transparency level between these two samples.

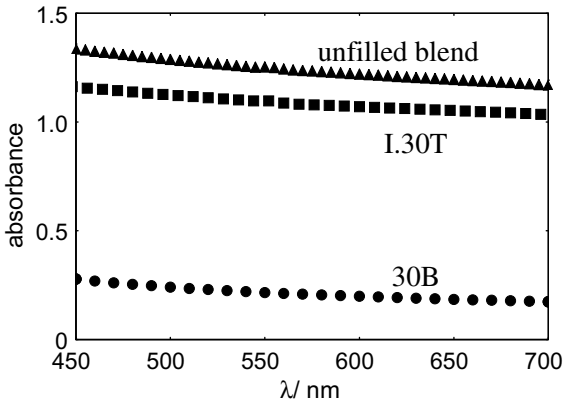

Fig. 5. Light absorbance of the unfilled blend (triangles), the 5 wt% I.30T (squares) and the 5 wt% 30B nanocomposites (circles) at room temperature (sample thickness = 0.15 cm).

from unfilled blend. A dramatic modification of the distribution of the PEO is induced by 30B (Figs. 6c and 7c), and at the same time, only minor changes were obtained for I.30T filled sample (Figs. 6b and 7b). These observations reveal a high sensitivity of the self-organization of the polymer components, with respect to the nature of the embedded nanoparticles. Favorable or unfavorable local interactions (clay surfactant groups-polymer entities) are reflected to the mesostructural topography of the nanocomposites, by promoting the mutual adhesion of the immiscible polymer pair.

Microscopy observations are also consistent with the rheological behavior reported above. Clay 30B interacts more favorably with PEO compared to I.30T, enhancing the viscosity of the minor phase and, thus, promoting the distribution of PEO droplets within the blend. A remarkable correlation between the macroscopically observed properties (rheological response and transparency) and the microscopy images can be established. The iPP/PEO blend coupled with 30B clay exhibits stronger viscoelasticity and an increased level of transparency compared to I.30T filled blend. At the same time, PEO droplets in iPP/PEO-30B blend are smaller.

A brief account of the possible underlying mechanisms for the effects of nanoclay addition to immiscible polymer blends is given below. The shrinkage of the suspended droplets within the continuum of the major polymeric phase has been explained in terms of kinetics and/or thermodynamics. Based on the kinetic approach, the unequal distribution of the clay platelets between the two components of the polymer blends (as a consequence of the significant differences in the physico-chemical characteristics in a typical pair of incompatible polymers) leads to an increased viscosity of the preferentially clay enriched phase. The preferentially clay enriched phase can perturb the coalescence of the droplets, by imposing greater constrains to the diffusive motion of the second phase. For the specific system examined here, clay 30B preferentially

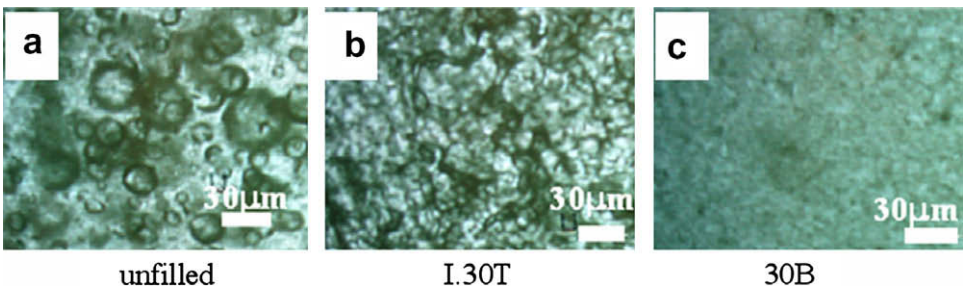

Fig. 6. Optical micrographs of the unfilled blend and the 5 wt% nanocomposite samples as indicated.

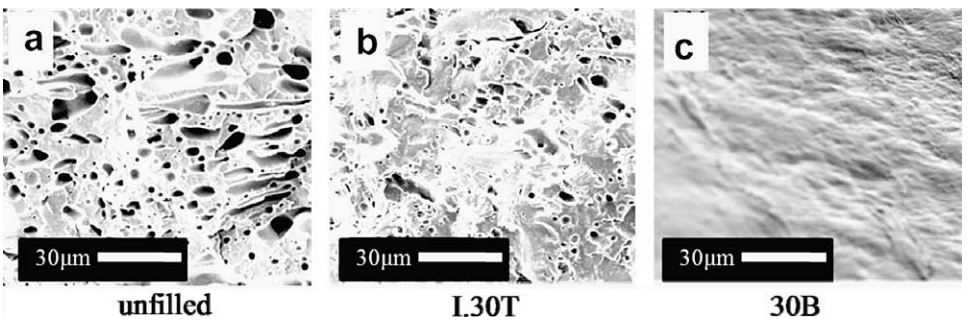

Fig. 7. SEM images of the unfilled blend and the 5 wt% nanocomposite samples as indicated.

enriches PEO, while I.30T interacts comparably with the two components.

The thermodynamic approach considers the changes of the free energy of mixing induced by the inclusion of nanoclay as a third component to the system. Increased concentration of silicate layers along the polymer–polymer interface can lower the interfacial tension and, thus, can promote the mutual adhesion and improve the wetting between the two polymeric components of the matrix. The proportionality between domain size and interface tension has been empirically shown for immiscible fluids [23]. The two mechanisms can act in parallel and synergistically so that their relative contributions to the overall morphology cannot be precisely evaluated. TEM imaging was used to demonstrate the dual positioning of clays tactoids to both polymer–polymer interface and in the bulk for PVDF/N-6 blends, thus revealing the double function of added clay as both compatibilizer and nanofiller [13].

In conclusion, we report on a unique nanocomposite blend based on a polymer blend matrix, in which the optical transparency is solely induced by appropriate organically modified nanoclays. Addition of nanoclays to a polymer blend can enable precise tuning of the domain sizes and, by doing so, can modify a series of macroscopically observed material properties of the hybrid system. Strong interactions in the organic/inorganic interface can drastically alter the topological parameters of the binary matrix, by preventing the clustering of the dispersed domains, to such an extent that the system appears completely transparent. To our knowledge, it is the first time that the emulsifying efficiency of nanoclays to polymer blends can be documented by bare eye.

Appendix A. Table of contents

We report on the effects of added nanoclay to the topological characteristics and the macroscopic properties of a polymer blend consisting of isotactic polypropylene (iPP) as the major component and poly(ethylene oxide) (PEO) as the minor component. A drastic reduction of the domain size of PEO within the continuum of iPP, as a consequence of incorporation of organically modified nanoclay, leads to a dramatic transformation from an opaque to a transparent system. This effect is demonstrated in the Figure below.

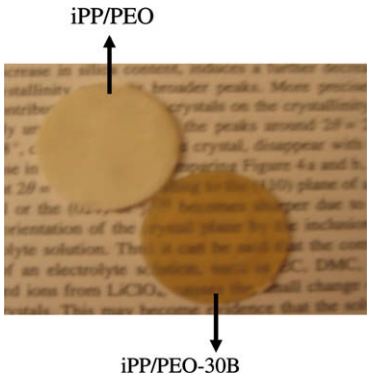

References

[1] Lim SK, Kim JW, Chin J, Kwon YK, Choi HJ. Chem Mater 2002;14:1989.
[2] Voulgaris D, Petridis D. Polymer 2002;43:2.
[3] Gelfer MY, Song HH, Liu L, Hsiao BS, Chu B, Rafailovich M, et al. J Polym Sci B Polym Phys 2003;41:44.
[4] Wang Y, Zhang Q, Fu Q. Macromol Rapid Commun 2003;24:231.
[5] Ray SS, Pouliot S, Bousima M, Utracki LA. Polymer 2004;45:8403.
[6] Li Y, Shimizu H. Polymer 2004;45:7381.
[7] Khatua BB, Lee DJ, Kim HY, Kim JK. Macromolecules 2004;37:2454.
[8] Yoo Y, Park C, Lee SG, Choi KY, Kim DS, Lee JH. Macromol Chem Phys 2005;206:878.
[9] Ray SS, Bousmina M. Macromol Rapid Commun 2005;26:1639.
[10] Yurekli K, Karim A, Amis EJ, Krishnamoorti R. Macromolecules 2003;36:7256.
[11] Yurekli K, Karim A, Amis EJ, Krishnamoorti R. Macromolecules 2004;37:507.
[12] Kelarakis A, Giannelis EP, Yoon K. Polymer 2007;48:7567.
[13] Vo LT, Giannelis EP. Macromolecules 2007;40:8271.
[14] (a) Kelarakis A, Yoon K, Sics I, Somani RH, Hsiao BS, et al. Polymer 2005;46:5103;
(b) Kelarakis A, Yoon K, Sics I, Somani RH, Chen X, Hsiao BS, et al. J Macromol Sci B Phys 2006;45:247.
[15] Frensch H, Jungnickel BJ. Colloid Polym Sci 1989;267:16.
[16] Aranda P, Ruiz-Hitzy E. Chem Mater 1992;4:1395.
[17] Loyens W, Jannasch P, Maurer FHJ. Polymer 2005;46:903.
[18] Strawhecker KE, Manias E. Chem Mater 2003;15:844.
[19] Gadjourova Z, Andreev YG, Tunstall DP, Bruce PG. Nature 2001;412:520.
[20] Krishnamoorti R, Giannelis EP. Macromolecules 1997;30:4097.
[21] Kelarakis A, Yoon K, Somani RH, Chen X, Hsiao BS, Chu B. Polymer 2005;46:11591.
[22] Krishnamoorti R, Yurekli K. Curr Opin Colloid Interface Sci 2001;6:464.
[23] Wu S. Polym Eng Sci 1987;27:335.